



Contents lists available at ScienceDirect

## Arabian Journal of Chemistry

journal homepage: [www.ksu.edu.sa](http://www.ksu.edu.sa)

Original article

## Interaction of xanthoxyletin with protein, molecular docking and antitumor activity in human chronic myeloid leukemia K562 cells

Chen Wang<sup>a,1,\*</sup>, Zhijie You<sup>a,1</sup>, Yihui He<sup>a,1</sup>, Siqi Chen<sup>a</sup>, Xin Chen<sup>a</sup>, Shuang Qu<sup>b</sup>, Ning Zhao<sup>c</sup>, Xin Chen<sup>a,\*</sup><sup>a</sup> Department of Pathology, Shengli Clinical Medical College of Fujian Medical University, Fujian Provincial Hospital, Fuzhou University Affiliated Provincial Hospital, Fuzhou 350001, Fujian, China<sup>b</sup> Department of Hematology, Department of Pathology, Shengli Clinical Medical College of Fujian Medical University, Fujian Provincial Hospital, Fuzhou University Affiliated Provincial Hospital, Fuzhou 350001, Fujian, China<sup>c</sup> National Key Laboratory of Intelligent Tracking and Forecasting for Infectious Diseases, National Institute for Communicable Disease Control and Prevention, Chinese Center for Disease Control and Prevention, Beijing 102206, China

## ARTICLE INFO

## Keywords:

Xanthoxyletin  
Interaction  
Hemoglobin  
Human chronic myeloid leukemia K562

## ABSTRACT

Xanthoxyletin (C<sub>15</sub>H<sub>14</sub>O<sub>4</sub>), a natural linear pyranocoumarin, is known to trigger anti-cancer activities, although its anticancer mechanisms are largely unknown. Human hemoglobin (HHb) as a major plasma protein could play a key role in the transportation and biodistribution of therapeutic molecules. In this study, the interaction of xanthoxyletin with HHb was measured under physiological conditions using multi-spectroscopic techniques along with molecular docking simulation. Also, the interaction of xanthoxyletin with human chronic myeloid leukemia K562 cells was assessed by cellular assays. It was deduced that each xanthoxyletin molecule shows a thermodynamically favorable interaction with one molecule of HHb with a binding constant (K<sub>b</sub>) in the orders of 10<sup>3-4</sup> M<sup>-1</sup>. These interactions did not significantly result in the loss of α-helical content of HHb. In silico studies supported the experimental findings and demonstrated that non-covalent forces including hydrogen bonds (Ala88 and Arg92), pi-pi stacking (Trp37), and hydrophobic interactions (and Pro95 and Pro36) are the main forces contributing to the xanthoxyletin-HHb complex formation. Cellular and molecular assays showed that xanthoxyletin mitigated the proliferation of K562 cells through apoptosis induction mediated by overexpression of p53, caspase-3, and PARP cleavage. This data may hold great promise for the development of anticancer compounds with potential blood protein binding stemming from xanthoxyletin derivatives/hybrids.

## 1. Introduction

According to reports, leukemia is an anomaly caused by the deregulation of the equilibrium between the blood cells' proliferative and differentiating processes (Sawyers 1999). Chemotherapy has been appointed as the first option for patients suffering from chronic myelogenous leukemia (CML). However, the appearance of multidrug resistance in CML (Ünlü, Kiraz et al. 2014) has convinced researchers to explore the chemo-free treatment paradigm (Scheffold and Stilgenbauer 2020).

Recently, natural-based compounds, with growing scientific interest, have been extensively investigated in the prevention and treatment of

leukemia (Goel, Kumar et al. 2023). They not only show potential plasma protein binding properties but also demonstrate anticancer activity with fewer adverse effects against off-target tissues.

Coumarins and their derivatives/hybrids as a crucial group of plant-based substances with pharmacological properties have been widely used in the development of anti-cancer systems (Önder 2020, Bhattarai, Kumbhar et al. 2021, Shaik, Katari et al. 2023). Xanthoxyletin (C<sub>15</sub>H<sub>14</sub>O<sub>4</sub>) with an IUPAC name of 5-methoxy-2,2-dimethylpyrano[3,2-g]chromen-8-one is known as a linear pyranocoumarin with anti-cancer properties (Rasul, Khan et al. 2011) which is presented in several species such as *Zanthoxylum dipetalum* (Fish, Gray et al. 1975), *Zanthoxylum elephantiasis* (Tomko, Awad et al. 1968), and other organisms. However,

\* Corresponding authors at: Department of Pathology, Shengli Clinical Medical College of Fujian Medical University, Fujian Provincial Hospital, Fuzhou University Affiliated Provincial Hospital, Address: No.134 East Street, Gulou District, Fuzhou 350001, Fujian, China.

E-mail addresses: [l-morning@fjmu.edu.cn](mailto:l-morning@fjmu.edu.cn) (C. Wang), [cxc1210@fjmu.edu.cn](mailto:cxc1210@fjmu.edu.cn) (X. Chen).

<sup>1</sup> The authors contributed equally to the articles.

<https://doi.org/10.1016/j.arabjc.2024.106015>

Received 5 August 2024; Accepted 6 October 2024

Available online 10 October 2024

1878-5352/© 2024 The Authors. Published by Elsevier B.V. on behalf of King Saud University. This is an open access article under the CC BY-NC-ND license (<http://creativecommons.org/licenses/by-nc-nd/4.0/>).

its anti-cancer effects on human CML and associated mechanisms remain unknown.

Additionally, a proper investigation into the anti-cancer efficacy of plant-based substances needs to carefully take into account both pharmacokinetic and pharmacodynamic characteristics, which contribute to the safety and potency of drugs (Schmidt, Gonzalez et al. 2010). Therefore, exploring the binding properties of xanthoxyletin with plasma protein can provide useful information about its pharmacokinetic and pharmacodynamic properties (Schmidt, Gonzalez et al. 2010). The potency of a drug and, consequently, its clinical efficacy can be significantly influenced by the plasma protein binding (Chen, Luo et al. 2021). The human hemoglobin (HHb) molecule as a carrier protein can interact with drugs and mediate their delivery/transport to the selective tissue (Chen, Luo et al. 2021). Hence, several studies have reported the interaction of plant-based compounds with hemoglobin using different experimental and theoretical analyses (Chaudhuri, Chakraborty et al. 2011, Sett, Paul et al. 2022, Luo, Wang et al. 2023, Ma, Sheng et al. 2023). As a result, to fully realize the bioavailability and distribution of xanthoxyletin, it is crucial to investigate how it may interact with HHb.

Therefore, in order to assess the pharmacokinetic properties as well as the potential of xanthoxyletin as an anti-cancer agent, we aimed to evaluate its interaction with HHb and human chronic myeloid leukemia K562 cells with a focus on one of the underlying mechanisms mediated by p53-caspase-3- Poly (ADP-ribose) polymerase pathway.

## 2. Materials and methods

### 2.1. Materials

Lyophilized powder of human hemoglobin (HHb, CAS# 9008-02-0), 8-anilino-1-naphthalenesulfonic acid (ANS), MTT (3-(4,5-Dimethylthiazol-2-yl)-2,5-Diphenyltetrazolium Bromide), and phosphate-buffered saline (PBS) were ordered from Sigma-Aldrich (St. Louis MO, USA). Xanthoxyletin (CAS# 84-99-1, Purity: >98 % HPLC) was obtained from BioCrick Science Solution Specialist (Chengdu, Sichuan, People's Republic of China). Roswell Park Memorial Institute 1640 (RPMI 1640) and fetal bovine serum (FBS) were purchased from GIBCO® (Invitrogen, Grand Island, NY, USA). The solvents used were of analytical grade and were purchased from Merck (Darmstadt, Germany).

### 2.2. Interaction design study

After adding the xanthoxyletin (prepared in DMSO) into HHb solution (prepared in PBS, 10 mM, pH 7.4), the mixed solutions were allowed to equilibrate for 5 min at defined temperatures (298, 304, and 310 K) before performing spectroscopic measurements. All measurements were carried out with a low concentration of xanthoxyletin ( $\leq 10.0 \mu\text{M}$ ) to minimize noise signals stemming from inner-filter effect (Shi, Pan et al. 2017).

### 2.3. Fluorescence quenching study

The fluorescence spectra of HHb ( $3 \mu\text{M}$ ) were read on a Varian Cary Eclipse fluorescence spectrophotometer (Varian Inc., Palo Alto, USA). The scanning speed and wavelength of (excitation, slit 10.0 nm) were fixed at 2 nm/s and 280 nm, respectively. The emission spectra were read at a wavelength range of 290–400 nm (slit 10.0 nm). All the spectra were properly baseline-corrected. The concentrations of xanthoxyletin were set in the range of 1 to  $10 \mu\text{M}$ .

### 2.4. Surface hydrophobicity

The surface hydrophobicity of HHb was determined using ANS as a hydrophobicity-fluorescence marker as described previously (Dabbour, He et al. 2020). Briefly, the HHb dissolved in PBS (10 mM, pH 7.0) with a concentration of  $3 \mu\text{M}$  (4 ml) were added by different concentrations of

xanthoxyletin (1 to  $10 \mu\text{M}$ ). Then, the samples were mixed with ANS ( $20 \mu\text{l}$  of 8.0 mM, prepared in the same buffer), and incubated at room temperature for 5 min in the dark. The fluorescence intensity was quantified on a Cary Eclipse spectrophotometer (Varian Inc., Palo Alto, USA) with an excitation wavelength of 380 nm (slit 10.0 nm). The emission intensities were quantified at 485 nm. All the intensities were appropriately baseline-corrected.

### 2.5. Circular dichroism (CD) measurement

To measure xanthoxyletin-triggered secondary structural changes in HHb, CD spectra of free HHb or complex HHb were recorded. The CD scan range was set in the far-UV region, 190–250 nm. The spectra were read at room temperature on the Jasco-J820 Spectro-polarimeter. The protein samples were read using a quartz cell of 1 mm path length. HHb ( $3 \mu\text{M}$ ) was prepared in PBS (10 mM, pH 7.0) and the spectra were recorded at different concentrations of xanthoxyletin (1 to  $10 \mu\text{M}$ ). The mean residue ellipticity in  $\text{deg cm}^2\text{dmol}^{-1}$  was calculated as previously reported (Anwer, AlQumaizi et al. 2021).

### 2.6. Molecular docking study

The three-dimensional (3D) structure of xanthoxyletin was obtained from the PubChem database (CID 66,548 – PubChem). From the online protein data bank, the 3D structure of HHb having PDB ID = 7VDE was retrieved (<https://www.rcsb.org>). HHb was prepared for molecular docking simulation by removing native ligands, heme groups and water molecules while hydrogen atoms and Kollman charges were added using the Autodock tool. Autodock Vina version (1.2.0) was employed to carry out the blind molecular docking for xanthoxyletin with HHb (Grid center: 90x73x89). All other parameters were used as default. The resultant docked poses were analyzed to determine the amino acid residues and forces involved in the binding site using Visualizer.

### 2.7. Cell culture

Chronic myeloid leukemia K562 cells (Cell Bank of Shanghai Institute of Biochemistry & Cell Biology) were grown in RPMI 1640 culture medium containing 10 % FBS, 100 U/ml penicillin and 100 U/ml streptomycin in a  $\text{CO}_2$  incubator at  $37^\circ\text{C}$ .

### 2.8. MTT assay

K562 cell viability was assessed by MTT assay as described previously (Chun-Guang, Jun-Qing et al. 2010). Briefly, K562 cells seeded for 24 h were incubated with fresh RPMI 1640 medium containing 1, 5, 10, 50, and  $100 \mu\text{M}$  of xanthoxyletin for 48 h. Afterward, MTT (5 mg/ml) was added into each well for 4 h and the insoluble formazan was dissolved in dimethyl sulfoxide (DMSO, 0.5 %) for 15 min. The absorbance of the samples was detected at 492 nm on a microtiter plate reader (Bio-Rad, CA, USA).

### 2.9. Activation of caspase-9, –3 assay in vitro

The caspase activity was done using caspase-9, –3 activity assay kits (Beyotime Institute of Biotechnology, Shanghai, China) as described previously. Briefly, after obtaining total protein using total protein lysis buffer (Beyotime Institute of Biotechnology, Shanghai, China) and calculating the protein concentration on BCA protein assay kit (Sigma-Aldrich, St. Louis MO, USA) from xanthoxyletin –incubated or control K562 cells, caspase-9, –3 activity assay was done. For this reason,  $10 \mu\text{L}$  of protein solution was mixed with  $80 \mu\text{L}$  of reaction buffer and  $10 \mu\text{L}$  of the substrate and incubated for 2 h at  $37^\circ\text{C}$ . The absorbance of the samples was read at 405 nm on a microtiter plate reader (Bio-Rad, CA, USA).

## 2.10. ELISA assay

After extraction of the total protein and determination of its concentration as described above, the total proteins were used for determination of expression of p53 (ab171571), caspase-9 (KA0185), caspase-3 (ab220655), and cleaved PARP (ab119690) according to Manufacturer's instructions provided by relevant ELISA Kits.

## 2.11. Statistical analysis

Some data are expressed as mean  $\pm$  SD and the differences among groups were determined with one-way analysis of variance (ANOVA). Differences were considered significant at  $P < 0.05$ .

## 3. Result and discussion

### 3.1. Fluorescence study

#### 3.1.1. Fluorescence quenching measurement

The intrinsic fluorescence measurement is typically used to analyze the interaction of small compounds with biomacromolecules, especially proteins (Weljie and Vogel 2002, Mátyus, Szöllősi et al. 2006). Therefore, to obtain detailed information about the interaction of xanthoxyletin with HHb intrinsic fluorescence measurement was done, HHb is comprised of 574 amino acids with two  $\alpha$   $\beta$  dimers in which three Trp amino acid residues per each  $\alpha$   $\beta$  dimer,  $\alpha$ -14 Trp,  $\beta$ -15 Trp,  $\beta$ -37 Trp, are responsible for the intrinsic fluorescence of HHb (Chen, Luo et al. 2021, Akram, Osama et al. 2023). But among other aromatic amino acids, the  $\beta$ -37 Trp is essentially the most fluorescent residue (Chen, Luo et al.

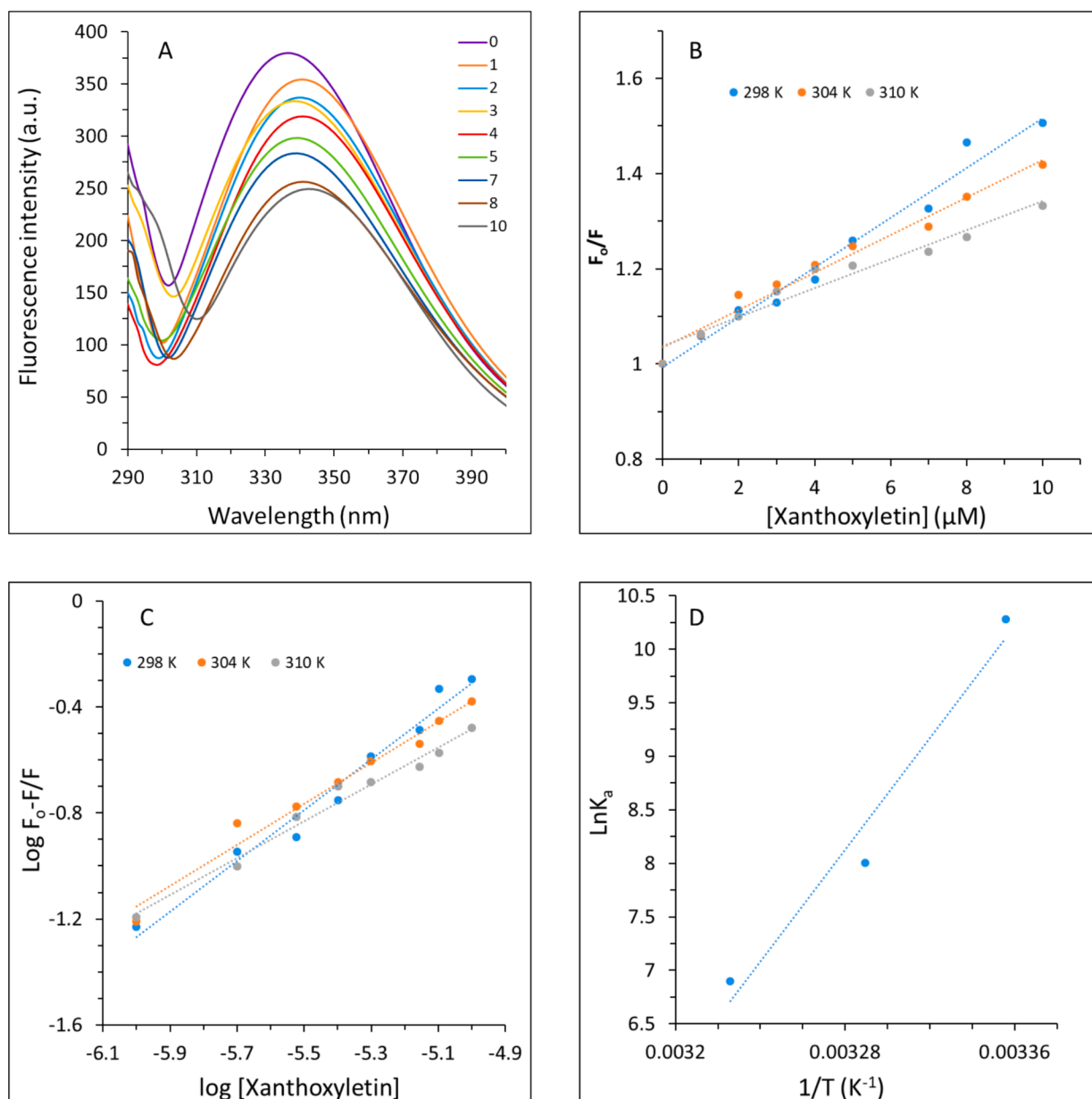


**Fig. 1.** Fluorescence spectroscopy study for analysis of the interaction of xanthoxyletin with HHb. (A) Fluorescence emission spectra of HHb without and with increasing concentrations of xanthoxyletin. The concentration of HHb was kept constant at 3  $\mu$ M and different concentrations (1–10  $\mu$ M) of xanthoxyletin were added.  $\lambda_{\text{ex}} = 280$  nm;  $\lambda_{\text{em}} = 290$ –400 nm. (B) The Stern–Volmer plots derived from the quenching study to calculate the quenching parameters. (C) The modified Stern–Volmer plots derived from the quenching study to calculate the binding parameters. (D) The van't Hoff's plot derived from the quenching study to calculate the thermodynamic parameters.

2021, Pant, Yadav et al. 2023). Fig. 1(A) displays the fluorescence emission spectra of HHb following the interaction with varying concentrations of xanthoxyletin. As revealed from the results, a continuous fluorescence quenching of HHb was observed with increasing concentrations of xanthoxyletin with a minor redshift in the maximum peak position. The fluorescence quenching of HHb disclosed the formation of the xanthoxyletin-HHb complex associated with minor changes in the tertiary structure of HHb, which may slightly increase the accessibility of the solvent to HHb (Panchal, Sehrawat et al. 2023). The mode of fluorescence quenching was then investigated using the Stern–Volmer equation (Panchal, Sehrawat et al. 2023).

$$F_0/F = 1 + K_{sv}[xanthoxyletin] = 1 + k_q\tau_0[xanthoxyletin] \quad (1)$$

Here,  $F_0$  and  $F$  are the fluorescence intensities in the absence and presence of xanthoxyletin, respectively.  $[xanthoxyletin]$  is the total concentration of the xanthoxyletin,  $K_{sv}$  is the Stern–Volmer quenching constant,  $k_q$  is the bimolecular quenching constant, and  $\tau_0$  defines the lifetime of the HHb in the excited state with a value of  $\sim 10^8 \text{ s}^{-1}$  (Panchal, Sehrawat et al. 2023).

The Stern–Volmer plot is demonstrated in Fig. 1(B) and the values calculated are summarized in Table 1. It was observed that  $K_{sv}$  values of the xanthoxyletin-HHb interaction ranged from 5.21 to  $3.0 \times 10^4 \text{ M}^{-1}$ .

Three modes of fluorescence quenching, static, dynamic and combined quenching, can determine the nature of the ligand–protein complex and the type of interaction (Abarova, Antonova et al. 2022). In dynamic fluorescence quenching, the ligand has enough energy for the interaction with the excited state fluorophore. While, in static quenching, the interaction between the ligand and fluorophore leads to the induction of a non-fluorescent ground state ligand–protein complex (Anwer, AlQumaizi et al. 2021). The mode of quenching that occurred in the formation of the xanthoxyletin-HHb complex was distinguished using the  $kq$  values.

The values of  $kq$  as a function of absolute temperature are mentioned in Table 1. The calculated  $k_q$  values ( $5.21$  to  $3.0 \times 10^{12} \text{ M}^{-1}\text{s}^{-1}$ ) were much greater than  $2.0 \times 10^{10} \text{ M}^{-1}\text{s}^{-1}$ , the maximum value for scatter collision of the biomacromolecule (Anwer, AlQumaizi et al. 2021). The values of  $k_q$  suggested that the non-fluorescent complex derived from a static quenching formed following interaction of xanthoxyletin with HHb (Zhao, Yao et al. 2023).

### 3.1.2. Binding and thermodynamics parameters

Fluorescence quenching results were further utilized to measure the affinity of xanthoxyletin to HHb using a modified Stern–Volmer equation (Anwer, AlQumaizi et al. 2021)

$$\log F_0 - F/F = \log Ka + n \log [xanthoxyletin] \quad (2)$$

Here,  $K_a$  and  $n$  are binding constant and the number of binding sites, respectively. The Modified Stern–Volmer plot is displayed in Fig. 1(C). The slope and y-axis intercept of this plot result in the calculation of  $n$  and  $K_a$  values, respectively (Table 2).

The logarithmic values of  $K_a$  ranged between 4.47 and 3.00 and the values of  $n$  values were in the range of 0.95–0.69. The findings suggested that the binding affinity decreased with increasing the temperature and indicated xanthoxyletin's lower affinity towards HHb at physiological temperature (310 K) in comparison with the lower temperatures. Also, a similar trend was observed with the values of  $n$ , revealing that there was

**Table 1**

The values of quenching constants for the interaction of xanthoxyletin and HHb at different temperatures.

pH	Temperature (K)	$K_{sv} (\times 10^4 \text{ M}^{-1})$	$K_q (\times 10^{12} \text{ M}^{-1} \text{ s}^{-1})$	R2
7.4	298	5.21	5.21	0.9777
	304	3.94	3.94	0.9745
	310	3.03	3.03	0.9492

**Table 2**

The values of binding constants for the interaction of xanthoxyletin and HHb at different temperatures.

pH	Temperature (K)	$\log K_a$	$n$	R2
7.4	298	4.47	0.95	0.9777
	304	3.48	0.77	0.9745
	310	3.00	0.69	0.9492

around one binding site on HHb per xanthoxyletin molecule, which behave in a negative cooperative manner,  $n < 1$ , (Li, Wang et al. 2014, Rahmani, Mogharizadeh et al. 2018).

The thermodynamic parameters of the xanthoxyletin-HHb interaction were measured to determine the major forces that contribute to the complexation of these two molecules. The values of thermodynamic parameters as well as their negative or positive signs play key roles in the determination of the binding forces contributing to this complexation. In general, ligand and macromolecule interactions are typically dictated by non-covalent forces including hydrogen bonds, hydrophobic and electrostatic interactions as well as van der Waals forces (Anwer, AlQumaizi et al. 2021). The values of enthalpy change ( $\Delta H^\circ$ ) and entropy change ( $\Delta S^\circ$ ) were calculated using van't Hoff's equation (Anwer, AlQumaizi et al. 2021):

$$\ln K_a = -\Delta H^\circ / RT + \Delta S^\circ R \quad (3)$$

Here,  $R$  is the universal gas constant and  $T$  is the absolute temperature. The corresponding van't Hoff's plot is shown in Fig. 1(D) and the calculated values of  $\Delta H^\circ$  and  $\Delta S^\circ$  are given in Table 3.

A negative value of  $\Delta S^\circ$  signifies that that water molecules are randomly distributed around HHb following the binding of xanthoxyletin (Ross and Subramanian 1981, Das, Hazarika et al. 2020). Moreover, the positive value of  $\Delta H^\circ$  confirms the exothermic nature of the interaction between xanthoxyletin and HHb (Ross and Subramanian 1981, Bawa, Deswal et al. 2022). Negative values of both  $\Delta H^\circ$  and  $\Delta S^\circ$  are the evidence of the contribution of hydrogen bonds and van der Waals interaction (Ross and Subramanian 1981, Bawa, Deswal et al. 2022). Gibb's free energy ( $\Delta G^\circ$ ) was then calculated using the following (Anwer, AlQumaizi et al. 2021):

$$\Delta G^\circ = -\Delta H - T\Delta S^\circ \quad (4)$$

It was revealed that the values of  $\Delta G^\circ$  were in the range of  $-24.99$  to  $-17.27 \text{ kJ/mol}$  (Table 3), confirming the spontaneity of the xanthoxyletin-HHb interaction (Anwer, AlQumaizi et al. 2021).

### 3.2. Surface hydrophobicity, tertiary and secondary structural change studies

The hydrophobicity of macromolecules is based on the reaction of water molecules repulsed by nonpolar moieties caused by protein structural changes (Dabbour, He et al. 2020). The hydrophobic changes of protein can be assessed by the ANS probe as a marker, which more interrelates with the nonpolar portion of proteins (Dabbour, He et al. 2020). ANS fluorescence measurement then can be used as a potential characteristic in analyzing the tertiary structural changes in protein which are mediated by interacting with hydrophobic groups on the surface of the protein molecules (Dabbour, He et al. 2020, Jiang, Hu et al. 2023). ANS fluorescence intensities of free HHb and complexed

**Table 3**

The values of thermodynamic parameters for the interaction of xanthoxyletin and HHb at different temperatures.

pH	Temperature (K)	$\Delta H^\circ$ (kJ/mol)	$\Delta S^\circ$ (J/mol K)	$\Delta G^\circ$ (kJ/mol)
7.4	298	-216.50	-642.66	-24.99
	304			-21.13
	310			-17.27

HHb with xanthoxyletin were exhibited in Fig. 2A. ANS fluorescence intensity values of HHb treated with 1, 2, 3, and 4  $\mu\text{M}$  xanthoxyletin were comparable with the control group. In contrast, ANS fluorescence intensity values were more than that of the control ( $p < 0.05$ ) when the HHb samples interacted with 5, 7, 8, and 10  $\mu\text{M}$  xanthoxyletin. The increased ANS fluorescence intensity values of HHb upon interaction with 5, 7, 8, and 10  $\mu\text{M}$  xanthoxyletin demonstrated that the molecules of HHb are unfolded to some extent following the xanthoxyletin interaction. This could be because xanthoxyletin weakens the hydrogen bonds and hydrophobic forces on the surface of HHb, exposing hydrophobic regions hidden inside the protein (Ding, Han et al. 2010, Jiang, Hu et al. 2023).

CD spectroscopy is known as an important tool to detect the secondary ( $\alpha$ -helix,  $\beta$ -sheets,  $\beta$ -turn, and random coil) structural changes of protein after interaction with ligands (Jiang, Hu et al. 2023). To find out how xanthoxyletin interaction influences the  $\alpha$ -helix structure of HHb, the CD spectra of HHb with different concentrations of xanthoxyletin were monitored as depicted in Fig. 2B. Obviously, HHb's CD signal intensity tended to have two minima around 208 nm and 222 nm, revealing a substantial content of  $\alpha$ -helix structure (Simon and Cantor 1969, Precupas, Leonties et al. 2022). However, the CD spectral intensity of HHb reduced slightly following the interaction with xanthoxyletin. The secondary structure contents of HHb and the xanthoxyletin-HHb were then calculated using relevant CD software (Fig. 2B). The findings revealed that the secondary structure content of HHb altered slightly after the addition of xanthoxyletin. The  $\alpha$ -helix content decreased from 59.31 % to 58.99 %, 57.09 %, and 56.29 %, after interaction of HHb with 1, 5, and 10  $\mu\text{M}$  xanthoxyletin, confirming partial secondary structural perturbations in HHb structure (Ma, Sheng et al. 2023) after xanthoxyletin binding.

### 3.3. Molecular docking study

The interaction between xanthoxyletin and HHb was investigated theoretically to further verify experimental outcomes. Therefore, the probable binding site(s) and different interactions between xanthoxyletin (Fig. 3A) and HHb (Fig. 3B) were analyzed. The molecular docking analysis demonstrated potential binding energy to be  $-32.63$  kJ/mol, which signifies a moderate interaction between xanthoxyletin

and HHb. The binding energy calculated by theoretical analysis ( $-32.63$  kJ/mol) was significantly higher than that determined by the fluorescence quenching study ( $-24.99$  kJ/mol), revealing that the presence of heme and water molecules excluded in the theoretical analysis may have a key role in the binding affinity of HHb toward xanthoxyletin. The plausible binding site derived from minimum docking energy between xanthoxyletin and HHb is represented in Fig. 3C (i, ii). Also, the amino acid residues present in the binding site are shown in Fig. 3D (i, ii). As shown in Fig. 3C, xanthoxyletin tends to interact with Chains A, C, and D of HHb. Fig. 3D showed that different amino acids, including His87, Ala88, Arg92, Val93, Pro95, Thr134, Thr137, Ser138, and Lys139 in Chain A; Lye127 in chain C; and Val34, Pro36, Trp37 in chain D located in the binding site of HHb following the interaction with xanthoxyletin. Also, it was observed [Fig. 3D (i, ii)] that Ala88 and Arg92 formed hydrogen bonds between xanthoxyletin and HHb; Trp37 contributed to the formation of pi-pi stacking between aromatic rings of xanthoxyletin and HHb; and Pro95 and Pro36 formed hydrophobic forces between xanthoxyletin and HHb.

These findings correlated with fluorescence quenching spectroscopy that xanthoxyletin led to the fluorescence quenching of HHb. Also, experimental results showed that hydrogen bond and van der Waals forces could be involved in the interaction of xanthoxyletin and HHb. Theoretical study showed Ala88 and Arg92 are responsible for the formation of hydrogen bonds between xanthoxyletin and HHb, although hydrophobic forces also contribute to this interaction. Also, we may suggest that the pi-pi interaction between xanthoxyletin and Trp37 amino acid plays a key role in the fluorescence quenching and micro-environmental changes of Trp residue in HHb.

### 3.4. MTT assay

The effects of xanthoxyletin on the proliferation of K562 cancer cells were assessed using the MTT assay (Fig. 4A). It was shown that xanthoxyletin triggered an antiproliferative effect on the K562 cancer cell line in a concentration-dependent manner. The  $\text{IC}_{50}$  value of xanthoxyletin on the K562 cancer cell line was determined to be about 100  $\mu\text{M}$  after 48 h.

It has been reported previously that several monoterpenic coumarins from *Micromelum minutum* such as clauslactone E, minutin B and 8-

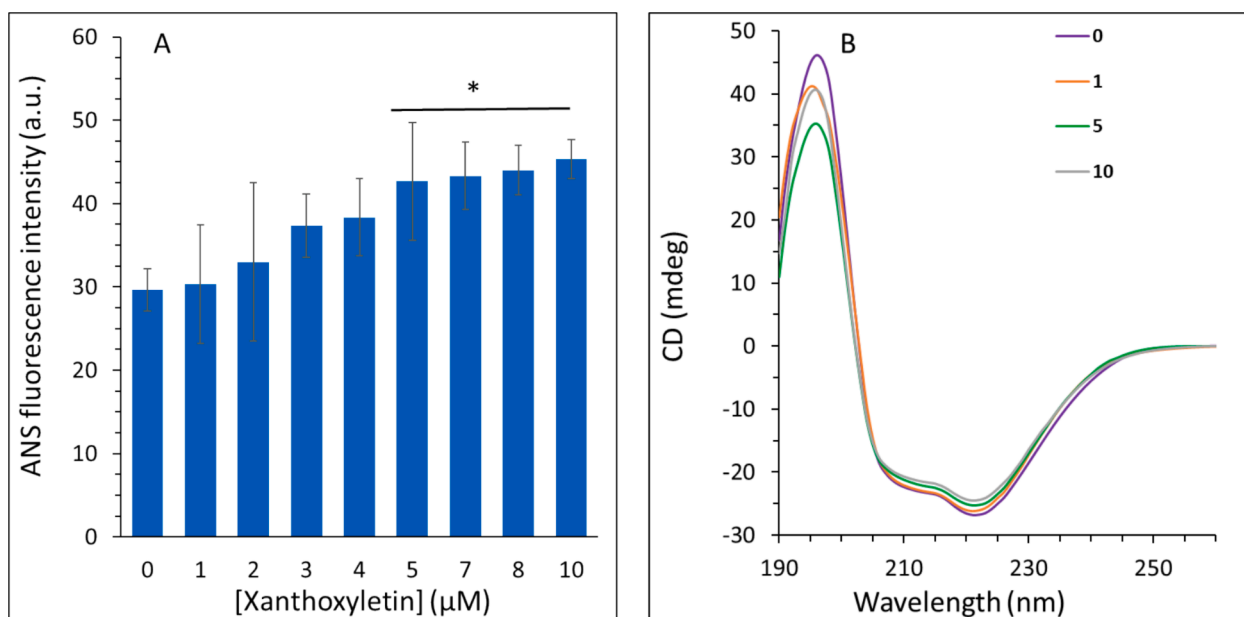
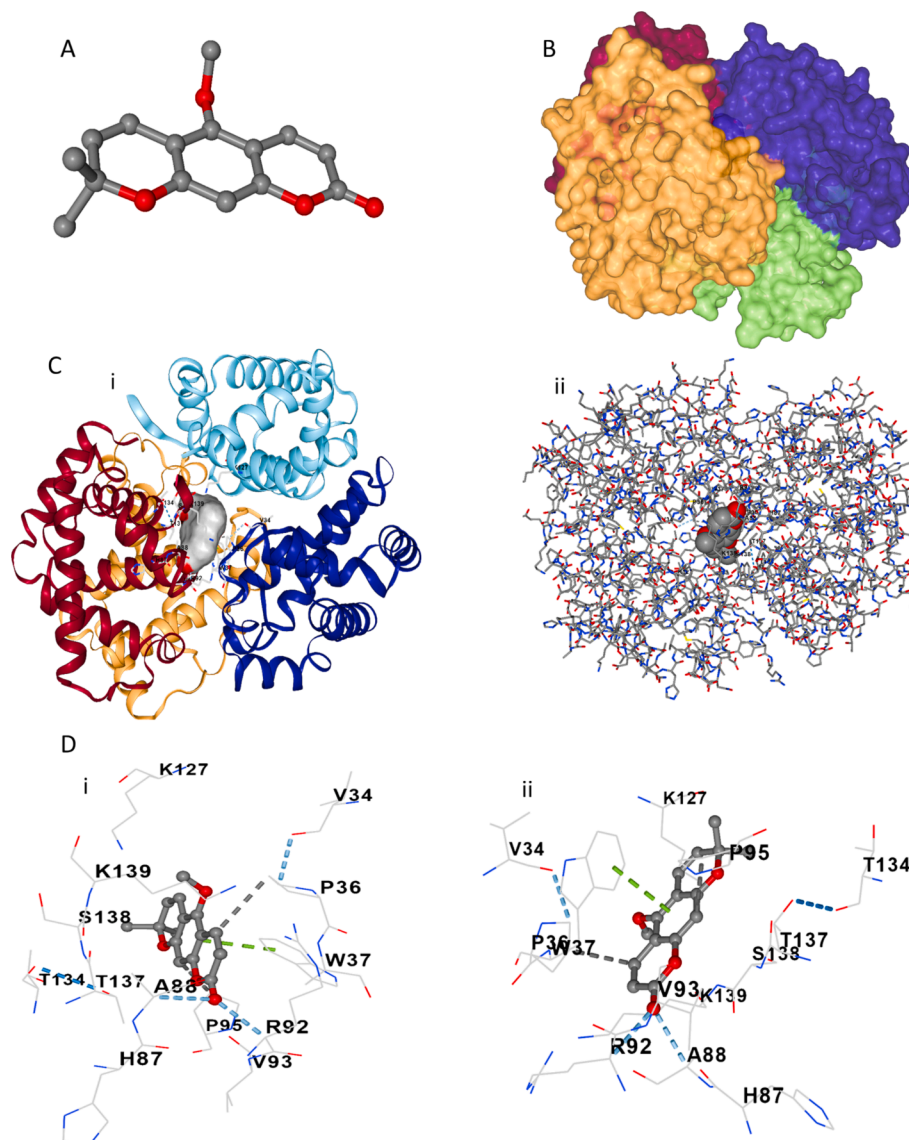


Fig. 2. Spectroscopy study for analysis of the interaction of xanthoxyletin with HHb. (A) ANS fluorescence emission spectra of HHb without and with increasing concentrations of xanthoxyletin. (B) Circular dichroism spectroscopy study for analysis of the interaction of xanthoxyletin with HHb. The concentration of HHb was kept constant at 3  $\mu\text{M}$  and different concentrations (1–10  $\mu\text{M}$ ) of xanthoxyletin were added.



**Fig. 3.** Molecular docking study for analysis of the interaction of xanthoxyletin with HHb. (A) xanthoxyletin structure. (B) HHb structure. (C) the docked xanthoxyletin-HHb complex with a ball-like structure (i) and amino acid residue-like structure. (D) Amino acid residues in the binding pocket with two rotational views.

hydroxyisocapnolactone-2',3'-diol show anti-cancer activity against the K562 cell line, with  $IC_{50}$  values of 12.1  $\mu$ M, 8.7  $\mu$ M and 16.9  $\mu$ M, respectively (Sakunpak, Matsunami et al. 2013). This data indicated that xanthoxyletin may have less potent activity in the K562 cell line relative to some other coumarin derivatives, which needs further analyses in future studies to combine or hybrid it with these derivatives to improve its anti-cancer activities.

### 3.5. Caspase activity assay

Although different *in vitro* and *in vivo* reports have investigated the pharmacotherapy of coumarin-based compounds in different types of cancers (Al-Warhi, Sabt et al. 2020, K peli Akkol, Gen et al. 2020), there is limited details regarding the elucidation of cellular and molecular pathways of the action of xanthoxyletin in human chronic myeloid leukemia cells. Therefore, the present study was designed to clarify one of the mechanisms of anti-cancer activity of xanthoxyletin in human chronic myeloid leukemia cell line (K562). To address this aim, to realize the probable mechanism of apoptosis-inducing effects triggered by xanthoxyletin, the expression levels of caspase-3 and caspase-9 that

play an important role in the intrinsic apoptosis pathway were assessed (Brentnall, Rodriguez-Menocal et al. 2013). Apoptosis as one of the main cell death-mediated pathways triggered by anticancer agents can be regulated by caspase-3 and caspase-9 overexpression (Brentnall, Rodriguez-Menocal et al. 2013). These two markers can serve as indicators of apoptosis stimulation since cleaved caspase-3 is present in apoptotic cells induced by both extrinsic and intrinsic cascades and caspase-9 mediates intrinsic pathway (Brentnall, Rodriguez-Menocal et al. 2013, Avrutsky and Troy 2021, Yadav, Yadav et al. 2021). To understand the probable mechanism of anti-cancer activity of xanthoxyletin, we analyzed caspase-3 and caspase-9 activity.

It was detected that exposure of K562 cells with xanthoxyletin with an  $IC_{50}$  concentration of 100  $\mu$ M could increase the caspase-9 activity (Fig. 4B) and caspase-3 activity (Fig. 4C) after 48 h incubation.

### 3.6. Protein expression levels

To further confirm the fact that xanthoxyletin incubation stimulates apoptosis through caspase-9, -3-mediated apoptosis, the expression levels of p53, cleaved caspase-9, cleaved caspase-3, and cleaved PARP

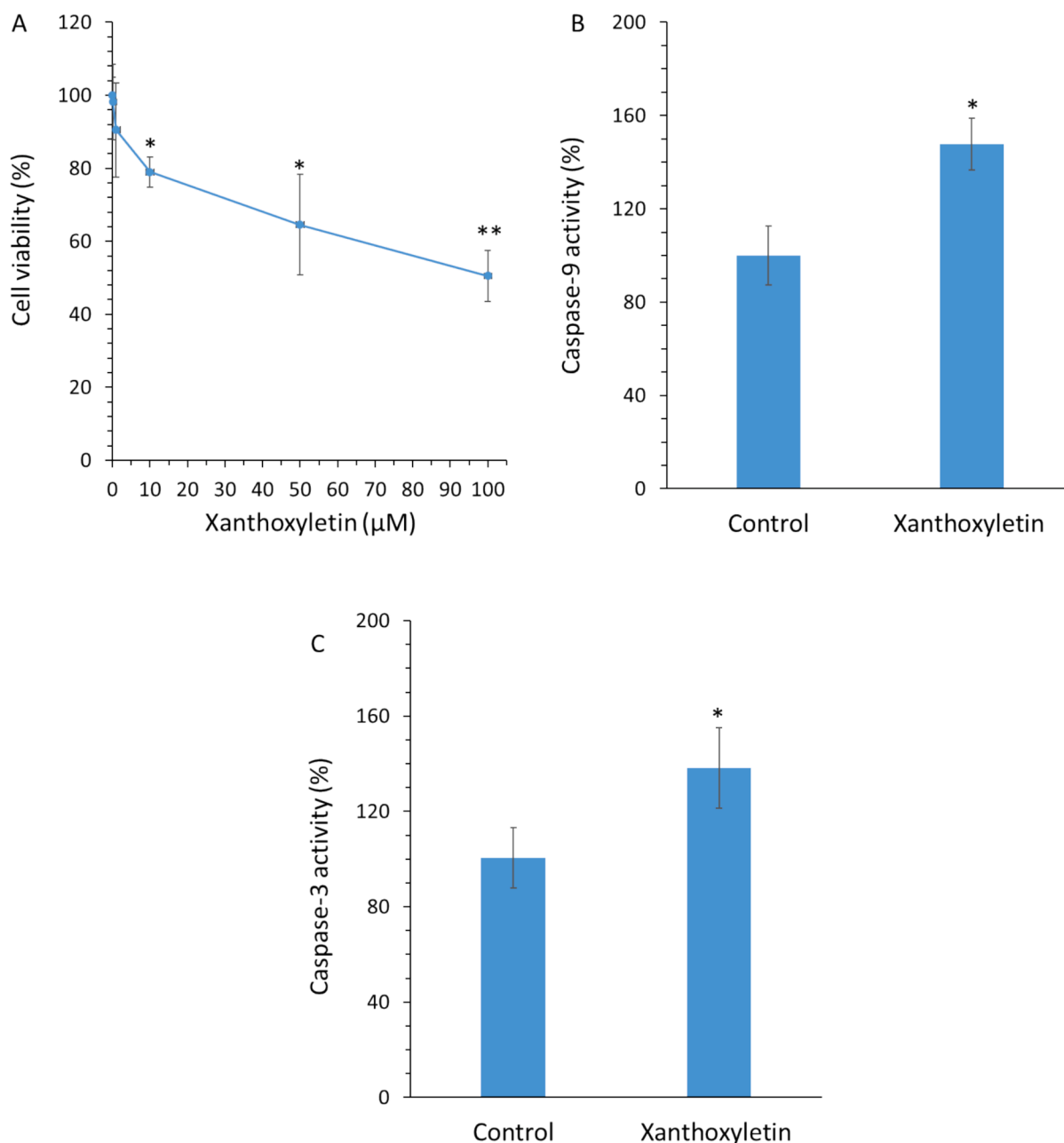


**Fig. 4.** (A) The effects of different concentrations of xanthoxyletin after 48 h on the proliferation of K562 cancer cells assessed by the MTT assay. The effect of  $\text{IC}_{50}$  value of xanthoxyletin (100  $\mu\text{M}$  after 48 h) on the (B) caspase-9 activity and (C) caspase-3 activity in the K562 cancer cell line. \* $p < 0.05$ ; \*\* $p < 0.01$  relative to control.

protein were assessed in the K562 cell using ELISA assay. When K562 cells were exposed to  $\text{IC}_{50}$  concentration of xanthoxyletin (100  $\mu\text{M}$ ), significant overexpression of p53, cleaved caspase-9, cleaved caspase-3, and cleaved-PARP proteins was observed (Fig. 5). It is well-documented that p53 could serve as a tumor suppressor marker and contribute to inhibiting tumor proliferation mediated by apoptosis and cell cycle arrest, while the overexpression of caspase-9, caspase-3 and their downstream target PARP regulated apoptosis through condensation of chromatin and fragmentation of DNA (Lim, Dorstyn et al. 2021). In the K562 cells, the expression of p53, cleaved caspase-9, cleaved caspase-3, and cleaved PARP was increased after xanthoxyletin treatment (Fig. 5).

Kimura et al. reported that natural xanthenes and coumarins extracted from species of the *Calophyllum* genus show potential anticancer activity against several types of cancer cells, especially K562 through the p53-mediated signaling pathway (Kimura, Ito et al. 2005).

Furthermore, it was shown that the combination of coumarin and anti-cancer doxorubicin could cause the induction of cell death in the K562 cells through apoptosis induction mediated by overexpression of the p53-caspase-3-PARP signaling pathway (Al-Abbas and Shaer 2021). The coumarin-based group as one of the most abundant moieties in nature can be regarded as a highly privileged group for the advancement of potential anticancer agents, as coumarin-based derivatives show the potential to regulate different signaling pathways in cancer cells (Song, Fan et al. 2020, Wu, Xu et al. 2020). In this paper, we showed that xanthoxyletin, a plant-derived coumarin could be used as a potential anticancer agent to show a direction for the design and development of promising coumarin-based compounds for clinical development in the control of leukemia.

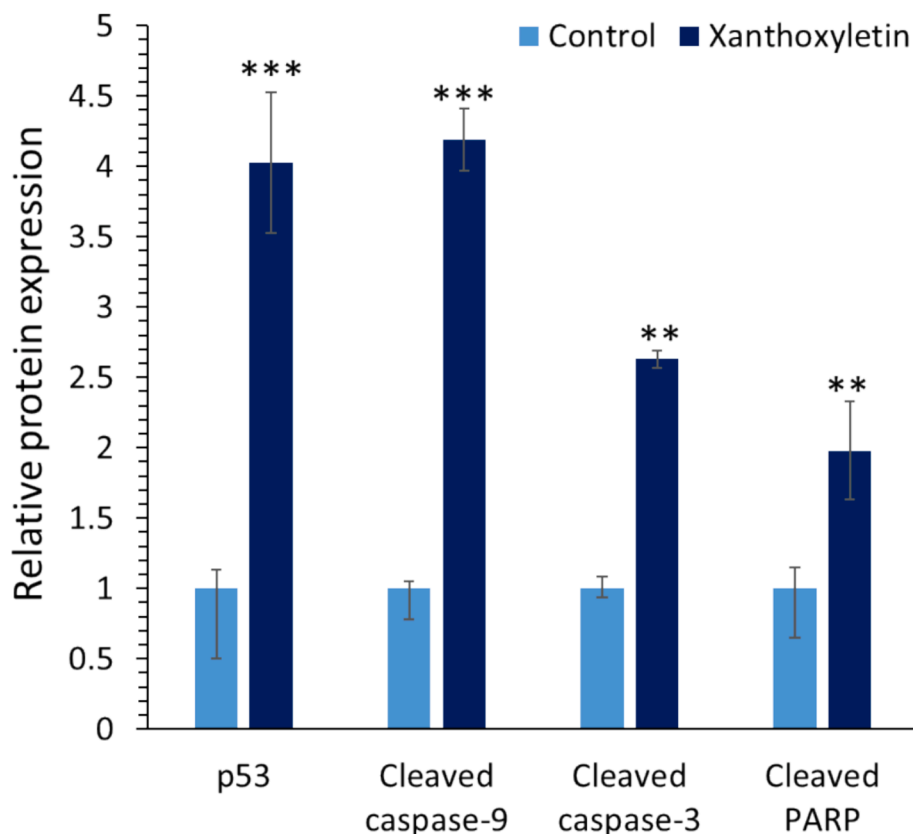


Fig. 5. The effect of IC<sub>50</sub> value of xanthoxyletin (100 μM after 48 h) on the protein expression in the K562 cancer cell line. \*\*p < 0.01; \*\*\*p < 0.001 relative to control.

#### 4. Conclusion

In conclusion, the interaction of xanthoxyletin with HHb was shown to be driven by a spontaneous reaction with a moderate binding affinity. Also, hydrogen bonds, van der Waals and hydrophobic forces contributed to the formation of the xanthoxyletin-HHb complex. Additionally, we found that xanthoxyletin had a negligible effect on the secondary structure of HHb while increasing the surface hydrophobicity and polarity around Trp 37 residues. Additionally, cellular and molecular assays revealed that xanthoxyletin was able to inhibit the proliferation of K562 cells in a concentration-dependent manner; elevate the caspase-9 and caspase-3 activity; and increase the expression of p53, cleaved caspase-9, cleaved caspase-3, and cleaved PARP. These results could provide useful information for the advancement of anti-cancer xanthoxyletin-based compounds with potential plasma protein binding affinity.

#### CRedit authorship contribution statement

**Chen Wang:** Conceptualization, Investigation, Methodology, Data curation, Analysis, Verification, Supervision, Funding, Software, Writing – original draft. **Zhijie You:** Conceptualization, Visualization, Investigation, Data curation, Analysis. **Yihui He:** Conceptualization, Visualization, Investigation, Data curation, Analysis. **Siqi Chen:** Conceptualization, Investigation, Writing – review & editing. **Xin Chen:** Conceptualization, Methodology, Data curation, Analysis. **Shuang Qu:** Conceptualization, Methodology, Data curation, Analysis. **Ning Zhao:** Conceptualization, Analysis, Writing – review & editing. **Xin Chen:** Conceptualization, Investigation, Data curation, Analysis, Verification, Supervision, Funding, Software, Writing – original draft.

#### Declaration of Competing Interest

The authors declare that they have no known competing financial interests or personal relationships that could have appeared to influence the work reported in this paper.

#### References

- Abarova, S., Antonova, B., Stoichkova, K., Nakova, N., Abarov, P., Zasheva, A., Koynova, R., Tenchov, B., 2022. Spectroscopic and thermodynamic characterization of the chemotherapy drug Epirubicin interaction with human serum albumin. *Bul. Chem. Commun.* 121.
- Akram, M., Osama, M., Lal, H., Hashmi, M.A., Anwar, S., 2023. Physicochemical evaluation of interaction behavior of a series of biocompatible gemini surfactants with hemoglobin: Insights from spectroscopic and computational studies. *Colloids Surf A Physicochem Eng Asp* 675, 132066.
- Al-Abbas, N.S., Shaer, N.A., 2021. Combination of coumarin and doxorubicin induces drug-resistant acute myeloid leukemia cell death. *Heliyon* 7 (3).
- Al-Warhi, T., Sabt, A., Elkaeed, E.B., Eldehna, W.M., 2020. Recent advancements of coumarin-based anticancer agents: An up-to-date review. *Bioorg. Chem.* 103, 104163.
- Anwer, R., AlQumaizi, K.I., Haque, S., Somvanshi, P., Ahmad, N., AlOsaimi, S.M., Fatma, T., 2021. Unravelling the interaction of glipizide with human serum albumin using various spectroscopic techniques and molecular dynamics studies. *J. Biomol. Struct. Dyn.* 39 (1), 336–347.
- Avrutsky, M.I., Troy, C.M., 2021. Caspase-9: a multimodal therapeutic target with diverse cellular expression in human disease. *Front. Pharmacol.* 12, 701301.
- Bawa, R., Deswal, N., Kumar, A., Kumar, R., 2022. Scrutinizing the interaction of bovine serum albumin and human hemoglobin with isatin-triazole functionalized rhodamine through spectroscopic and In-silico approaches. *J. Mol. Liq.* 360, 119558.
- Bhattarai, N., Kumbhar, A.A., Pokharel, Y.R., Yadav, P.N., 2021. Anticancer potential of coumarin and its derivatives. *Mini Rev. Med. Chem.* 21 (19), 2996–3029.
- Brentnall, M., Rodriguez-Menocal, L., De Guevara, R.L., Cepero, E., Boise, L.H., 2013. Caspase-9, caspase-3 and caspase-7 have distinct roles during intrinsic apoptosis. *BMC Cell Biol.* 14, 1–9.
- Chaudhuri, S., Chakraborty, S., Sengupta, P.K., 2011. Probing the interactions of hemoglobin with antioxidant flavonoids via fluorescence spectroscopy and molecular modeling studies. *Biophys. Chem.* 154 (1), 26–34.
- Chen, H.-B., Luo, C.-D., Ai, G.-X., Wang, Y.-F., Li, C.-L., Tan, L.-H., Lee, S.-M.-Y., Cheung, A.-K.-K., Su, Z.-R., Wu, X.-L., 2021. A comparative investigation of the

- interaction and pharmacokinetics of hemoglobin with berberine and its oxymetabolite. *J. Pharm. Biomed. Anal.* 199, 114032.
- Chun-Guang, W., Jun-Qing, Y., Bei-Zhong, L., Dan-Ting, J., Chong, W., Liang, Z., Dan, Z., Yan, W., 2010. Anti-tumor activity of emodin against human chronic myelocytic leukemia K562 cell lines in vitro and in vivo. *Eur. J. Pharmacol.* 627 (1–3), 33–41.
- Dabbour, M., He, R., Mintah, B., Golly, M.K., Ma, H., 2020. Ultrasound pretreatment of sunflower protein: Impact on enzymolysis, ACE-inhibition activity, and structure characterization. *J. Food Process. Preserv.* 44 (4), e14398.
- Das, S., Hazarika, Z., Sarmah, S., Baruah, K., Rohman, M.A., Paul, D., Jha, A.N., Roy, A. S., 2020. Exploring the interaction of bioactive kaempferol with serum albumin, lysozyme and hemoglobin: A biophysical investigation using multi-spectroscopic, docking and molecular dynamics simulation studies. *J. Photochem. Photobiol. B Biol.* 205, 111825.
- Ding, F., Han, B.-Y., Liu, W., Zhang, L., Sun, Y., 2010. Interaction of imidacloprid with hemoglobin by fluorescence and circular dichroism. *J. Fluoresc.* 20, 753–762.
- Fish, F., Gray, A.I., Waterman, P.G., 1975. Alkaloids, coumarins, triterpenes and a flavanone from the root of *Zanthoxylum dipetalum*. *Phytochemistry* 14 (9), 2073–2076.
- Goel, H., Kumar, R., Tanwar, P., Upadhyay, T.K., Khan, F., Pandey, P., Kang, S., Moon, M., Choi, J., Choi, M., 2023. Unraveling the therapeutic potential of natural products in the prevention and treatment of leukemia. *Biomed. Pharmacother.* 160, 114351.
- Jiang, S.-L., Hu, Z.-Y., Wang, W.-J., Hu, L., Li, L., Kou, S.-B., Shi, J.-H., 2023. Investigation on the binding behavior of human  $\alpha$ 1-acid glycoprotein with Janus Kinase inhibitor baricitinib: Multi-spectroscopic and molecular simulation methodologies. *Int. J. Biol. Macromol.* 125096.
- Kimura, S., Ito, C., Jyoko, N., Segawa, H., Kuroda, J., Okada, M., Adachi, S., Nakahata, T., Yuasa, T., Filho, V.C., 2005. Inhibition of leukemic cell growth by a novel anti-cancer drug (GUT-70) from *calophyllum brasiliense* that acts by induction of apoptosis. *Int. J. Cancer* 113 (1), 158–165.
- Küpelı Akkol, E., Genç, Y., Karpuz, B., Sobarzo-Sánchez, E., Capasso, R., 2020. Coumarins and coumarin-related compounds in pharmacotherapy of cancer. *Cancers* 12 (7), 1959.
- Li, X., Wang, G., Chen, D., Lu, Y., 2014. Binding of ascorbic acid and  $\alpha$ -tocopherol to bovine serum albumin: a comparative study. *Mol. Biosyst.* 10 (2), 326–337.
- Lim, Y., Dorstyn, L., Kumar, S., 2021. The p53-caspase-2 axis in the cell cycle and DNA damage response. *Exp. Mol. Med.* 53 (4), 517–527.
- Luo, X., Wang, Z., Xu, J., Gao, Z., Song, Z., Wang, W., 2023. Hemoglobin binding and antioxidant activity in spinal cord neurons: O-methylated isoflavone glycitein as a potential small molecule. *Arab. J. Chem.* 16 (10), 105164.
- Ma, Y., Sheng, J., Yan, F., Wei, W., Li, L., Liu, L., Sun, J., 2023. Potential binding of cryptotanshinone with hemoglobin and antimetastatic effects against breast cancer cells through alleviating the expression of MMP-2/-9. *Arab. J. Chem.* 105071.
- Mátyus, L., Szöllösi, J., Jenei, A., 2006. Steady-state fluorescence quenching applications for studying protein structure and dynamics. *J. Photochem. Photobiol. B Biol.* 83 (3), 223–236.
- Önder, A., 2020. Anticancer activity of natural coumarins for biological targets. *Stud. Nat. Prod. Chem.* 64, 85–109.
- Panchal, S., Sehrawat, H., Sharma, N., Chandra, R., 2023. Biochemical interaction of human hemoglobin with ionic liquids of noscapinoids: Spectroscopic and computational approach. *Int. J. Biol. Macromol.* 239, 124227.
- Pant, M., Yadav, M., Verma, A.K., Mahapatro, A.K., Roy, I., 2023. Comparative analysis of cobalt ferrite and iron oxide nanoparticles using bimodal hyperthermia, along with physical and in silico interaction with human hemoglobin. *J. Mater. Chem. B* 11 (21), 4785–4798.
- Precupas, A., Leonties, A.R., Neacsu, A., Angelescu, D.G., Popa, V.T., 2022. Bovine hemoglobin thermal stability in the presence of naringenin: Calorimetric, spectroscopic and molecular modeling studies. *J. Mol. Liq.* 361, 119617.
- Rahmani, S., Mogharizadeh, L., Attar, F., Rezayat, S.M., Mousavi, S.E., Falahati, M., 2018. Probing the interaction of silver nanoparticles with tau protein and neuroblastoma cell line as nervous system models. *J. Biomol. Struct. Dyn.* 36 (15), 4057–4071.
- Rasul, A., Khan, M., Yu, B., Ma, T., Yang, H., 2011. Xanthoxyletin, a coumarin induces S phase arrest and apoptosis in human gastric adenocarcinoma SGC-7901 cells. *Asian Pac J Cancer Prev* 12 (5), 1219–1223.
- Ross, P.D., Subramanian, S., 1981. Thermodynamics of protein association reactions: forces contributing to stability. *Biochemistry* 20 (11), 3096–3102.
- Sakunpak, A., Matsunami, K., Otsuka, H., Panichayupakaranant, P., 2013. Isolation of new monoterpene coumarins from *Micromelum minutum* leaves and their cytotoxic activity against *Leishmania major* and cancer cells. *Food Chem.* 139 (1–4), 458–463.
- Sawyers, C.L., 1999. Chronic myeloid leukemia. *N. Engl. J. Med.* 340 (17), 1330–1340.
- Scheffold, A., Stilgenbauer, S., 2020. Revolution of chronic lymphocytic leukemia therapy: the chemo-free treatment paradigm. *Curr. Oncol. Rep.* 22, 1–10.
- Schmidt, S., Gonzalez, D., Derendorf, H., 2010. Significance of protein binding in pharmacokinetics and pharmacodynamics. *J. Pharm. Sci.* 99 (3), 1107–1122.
- Sett, R., Paul, B.K., Guchhait, N., 2022. Deciphering the fluorescence quenching mechanism of a flavonoid drug following interaction with human hemoglobin. *J. Phys. Org. Chem.* 35 (3), e4307.
- Shaik, B.B., Katari, N.K., Seboletswe, P., Gundla, R., Kushwaha, N.D., Kumar, V., Singh, P., Karpoormath, R., Bala, M.D., 2023. Recent Literature Review on Coumarin Hybrids as Potential Anticancer Agents. *Anti-Cancer Agents in Medicinal Chemistry (formerly Current Medicinal Chemistry-Anti-Cancer Agents)* 23 (2), 142–163.
- Shi, J.-H., Pan, D.-Q., Jiang, M., Liu, T.-T., Wang, Q., 2017. In vitro study on binding interaction of quinapril with bovine serum albumin (BSA) using multi-spectroscopic and molecular docking methods. *J. Biomol. Struct. Dyn.* 35 (10), 2211–2223.
- Simon, S.R., Cantor, C.R., 1969. Measurement of ligand-induced conformational changes in hemoglobin by circular dichroism. *Proc. Natl. Acad. Sci.* 63 (1), 205–212.
- Song, X.F., Fan, J., Liu, L., Liu, X.F., Gao, F., 2020. Coumarin derivatives with anticancer activities: An update. *Arch. Pharm.* 353 (8), 2000025.
- Tomko, J., Awad, A.T., Beal, J.L., Doskotch, R.W., 1968. Isolation of candicine chloride, laurifoline chloride, and xanthoxyletin from the bark of *Zanthoxylum elephantiasis*. *J. Pharm. Sci.* 57 (2), 329–330.
- Ünlü, M., Kiraz, Y., Kaci, F.N., Özcan, M.A., Baran, Y., 2014. Multidrug resistance in chronic myeloid leukemia. *Turk. J. Biol.* 38 (6), 806–816.
- Weljie, A.M., Vogel, H.J., 2002. Steady-state fluorescence spectroscopy. *Calcium-Binding Protein Protocols: Volume 2: Methods and Techniques*. Springer 75–87.
- Wu, Y., Xu, J., Liu, Y., Zeng, Y., Wu, G., 2020. A review on anti-tumor mechanisms of coumarins. *Front. Oncol.* 10, 592853.
- Yadav, P., Yadav, R., Jain, S., Vaidya, A., 2021. Caspase-3: a primary target for natural and synthetic compounds for cancer therapy. *Chem. Biol. Drug Des.* 98 (1), 144–165.
- Zhao, Z., Yao, J., Li, H., Lan, J., Hollert, H., Zhao, X., 2023. Interaction of polystyrene nanoplastics and hemoglobin is determined by both particle curvature and available surface area. *Sci. Total Environ.* 899, 165617.